Accepted Article

Authors: Wenjing Hong, Xiaohui Li, Qingqing Wu, Jie Bai, Songjun Hou, Wenlin Jiang, Chun Tang, Hang Song, Xiaojuan Huang, Jueting Zheng, Yang Yang, Junyang Liu, Yong Hu, Jia Shi, Zitong Liu, Colin J. Lambert, and Deqing Zhang

This manuscript has been accepted after peer review and appears as an Accepted Article online prior to editing, proofing, and formal publication of the final Version of Record (VoR). This work is currently citable by using the Digital Object Identifier (DOI) given below. The VoR will be published online in Early View as soon as possible and may be different to this Accepted Article as a result of editing. Readers should obtain the VoR from the journal website shown below when it is published to ensure accuracy of information. The authors are responsible for the content of this Accepted Article.

WILEY-VCH

WILEY-VCH

RESEARCH ARTICLE

Structure-Independent Conductance of Thiophene-Based Single-Stacking Junctions

Xiaohui Li,[a]† Qingqing Wu,[b]† Jie Bai,[a]† Songjun Hou,[b] Wenlin Jiang,[c] Chun Tang,[a] Hang Song,[a] Xiaojuan Huang,[a] Jueting Zheng,[a] Yang Yang,[a] Junyang Liu,[a] Yong Hu,[a] Jia Shi,[a] Zitong Liu,[c]* Colin J. Lambert,[b]* Deqing Zhang,[c]* Wenjing Hong[a]*

Abstract: Intermolecular charge transport is crucial in π-conjugated materials but the experimental investigation remained challenging. Here, we show that charge transport through intermolecular and intramolecular paths in single-molecule and single-stacking thiophene junctions could be investigated using the mechanically controllable break junction (MCBJ) technique. We found that intermolecular charge transport ability through different single-stacking junctions is approximately independent of molecular structures, which contrasts with the strong length dependence of conductance in single-molecule junctions with the same building blocks, and the dominant charge transport path of molecules with two anchors transits from intramolecular to intermolecular paths when the conjugation pattern increased. The increase of conjugation further leads to higher binding probabilities due to the variation in binding energies supported by density functional theory (DFT) calculations. Our results demonstrate that intermolecular charge transport is not only the limiting step but also provides the efficient and dominate charge transport path at the single-molecule scale.

Introduction

The unique electronic properties of organic π-conjugated materials lead to various applications in flexible and stretchable, light-weight, ubiquitous devices for skin-like or wearable electronics, the Internet of Things and flexible displays *etc.*[1] Among the macroscopic π-conjugated materials, intermolecular charge transport is widely considered as the limiting step for the electronic processes[2] due to their weak dielectric constants, and

strong electron-phonon interactions, as well as the disordered microscopic structures. Despite substantial studies have been made to understand the intermolecular charge transport,[2d, 3] quantitative description of charge transport still remains challenging. Until now the insights of the charge transport are mostly from the theoretical calculations.[2a, 2c, 4] To investigate the role of intermolecular interactions in charge transport, the mechanically controllable break junction (MCBJ) studies have demonstrated that charge transport through intermolecular paths provides much lower conductance than that through intramolecular paths in oligophenylene ethynylenes (OPEs),[5] suggesting that the single-molecule break junction may offer new insight to overcome the long-pending challenges.

Among the π-conjugated materials, thiophene derivatives attracted intensive attention in organic electronic devices and molecular electronics owing to their outstanding electronic and optical properties.[6] Understanding the intrinsic charge transport through thiophene derivatives at the molecular level is essential for designing high-performance functional organic materials and devices. Until now, several groups have studied the intramolecular charge transport through thiophene derivatives based on its corresponding single-molecule junctions.[7] However, the intermolecular charge transport through thiophene derivatives, which plays a vital role in the ultimate charge-carrier mobility, has never been studied yet.

In this work, we investigated the intermolecular charge transport property in single-molecule and single-stacking thiophene junctions using the MCBJ technique. It is found that the thiophene molecules containing only one thiomethyl (-SMe) anchoring group can form single-stacking junctions with measurable conductance. Unexpectedly, the conductance of single-stacking junctions is approximately constant with the different conjugated pattern, while the probability to form single-stacking junctions improves by increasing the conjugation region, indicating the dynamic formation process provides the driving forces for their charge transport ability. Moreover, based on the detectable conductance of thiophene-based single-stacking junctions, we explored the intermolecular and intramolecular charge transport through thiophene derivatives at the single-molecule level, demonstrating the intermolecular and intramolecular charge transport can be distinguished and investigated upon MCBJ technique. We found that the intermolecular charge transport can be more efficient than intramolecular charge transport in thiophene derivatives and that the dominant charge transport path transitions from intramolecular to intermolecular when the conjugation increased. Our findings provide clear evidence that intermolecular, instead of intramolecular charge transport, could be the dominant conductance path for organic materials with large π-conjugated pattern.

[a]   X. H. Li, J. Bai, C. Tang, H. Song, X. J. Huang, J. T. Zheng, Y.
        Yang, J. Y. Liu, Y. Hu, J. Shi and Prof. W. J. Hong
        State Key Laboratory of Physical Chemistry of Solid Surfaces,
        iChEM, College of Chemistry and Chemical Engineering
        Xiamen University
        Xiamen, Siming South Road (China)
        E-mail: whong@xmu.edu.cn
[b]   Q. Q. Wu, S. J. Hou and Prof. C. J. Lambert
        Department of Physics
        Lancaster University
        Lancaster LA1 4YB (UK)
        E-mail: c.lambert@lancaster.ac.uk
[c]   W. L. Jiang, Z. T. Liu and D. Q. Zhang
        Beijing National Laboratory for Molecular Sciences, CAS Key
        Laboratory of Organic Solids, Institute of Chemistry
        Chinese Academy of Sciences
        Beijing, Zhongguancun North First Street 2 (China)
        E-mail: zitong_@iccas.ac.cn, dqzhang@iccas.ac.cn
[†]   These authors contributed equally to this work.

        Supporting information for this article is given via a link at the end of
        the document.

RESEARCH ARTICLE

Results and Discussion

Conductance measurement of the single-stacking junction.
The conductance of molecular junctions was characterized using MCBJ technique in solution (tetrahydrofuran:1,3,5-trimethylbenzene = 1:4, v/v) with/without 0.1 mM target molecules at a bias voltage of 0.1 V (Figure 1A). Briefly, the breaking and closing process between two electrodes was performed by the controllable bending of notched gold-wire chips. In this way, the molecular junctions were created by repeatedly breaking and forming the gold-gold atomic contacts. To investigate the charge transport through π-stacked thiophene dimer, molecule **S-T1** with only one -SMe terminal was employed to form a single-stacking junction via intermolecular interactions with each -SMe coupled to a gold electrode (Figure 1A).

Figure 1B shows several typical conductance-displacement traces of **S-T1** (red) and the solvent without molecules (black). Unlike in direct tunneling traces obtained for the solvent, the conductance indicated by the red traces decreases to two well-defined molecular plateaus after the rupture of the last gold-gold atomic contact at $1 G_0$ ($G_0 = 2e^2/h$),[8] suggesting the formation of two distinct molecular junctions for **S-T1**. The high conductance (H) and low conductance (L) plateaus can appear individually or together. To explore the correlation of the H and L states statistically, 2D cross-correlation analysis[9] is constructed (Figure S5A). A negatively correlated region centered at [$10^{-2.2}$ G_0, $10^{-4.0}$ G_0] and [$10^{-4.0}$ G_0, $10^{-2.2}$ G_0] is found for **S-T1**, indicating the two conductance states appear competitively in most cases (details in Supporting Information section 2). Then, one-dimensional (1D) conductance histogram was generated to determine the most likely conductance. As shown in Figure 1B, two evident conductance peaks are obtained. The H peak centered at $10^{-2.18\pm0.04}$ G_0 (517.1±44.0 nS) displays a narrow distribution and was 68 times higher than that of the L peak ($10^{-4.02\pm0.11}$ G_0, 7.5±2.0 nS) with a broad distribution. So, We speculated that the H peak corresponds to the single-molecule junctions bridged by -SMe[10] and thienyl[11] (upper panel in Figure 1A) and the L peak corresponds to the single-stacking junction through π-stacked dimers (bottom panel in Figure 1A). The broader peak width of the L peak is related to more degrees of freedom during the stretching process introduced by π-stacked dimers.

To reveal more information from the stretching process statistically, two-dimensional (2D) conductance histograms were constructed from collecting thousands of individual traces without data selection (Figure 1C). We note that the H intensity cloud maintains almost flat during the stretching process, while the slope of the L intensity cloud decreases significantly, suggesting that the conductance of single-stacking junction highly depends on the stacking configurations.[12] Besides, the stretching distance of H state is much shorter than L state (inset of Figure 1C). Considering the snap-back distance 0.5 nm[12] (details in Supporting Information section 2.1), the stretching distance of H state is 0.68 ± 0.03 nm, which is comparable with the **S-T1**

molecular length calculated from theoretical simulations (see Table S1). In comparison, the stretching distance of L state is almost twice than that of H state (1.31±0.02 nm), which is in accordance with single-stacking junction of **S-T1** dimer with longer length. To further verify our hypothesis, the electronic coupling types of two conductance states were confirmed by flicker noise analysis[13] (details in Experimental Section). As shown in Figure 1D, the noise power scales as $G^{1.1}$ for H state and as $G^{1.8}$ for L state, corresponding to through-bond coupling in the H state of single-molecule junctions and through-space coupling in the L state of single-stacking junctions, which agrees well with our hypothesis. The phenomenon is different to short oligothiophene with iodide anchors at both ends, which tend to lie flat on Au electrode and form single-molecule junctions through metal-π interactions, as reported by Xiang et al.[14] The possible reason is that the thiophene molecules with -SMe at only one side tend to stand on gold electrode rather than lie flat, thus facilitating the formation of a gold-S donor-acceptor bond by the S atom of the thiophene ring and the gold electrode during the stretching process, which is supported by the stretching distance and flicker noise analysis. These results indicate that the interactions between thiophene rings are strong enough to form the single-stacking junctions and the intermolecular charge transport ability of single-stacking junctions base on **S-T1** is much lower than that of corresponding single-molecule, as reported before in an OPEs sysem.[5a]
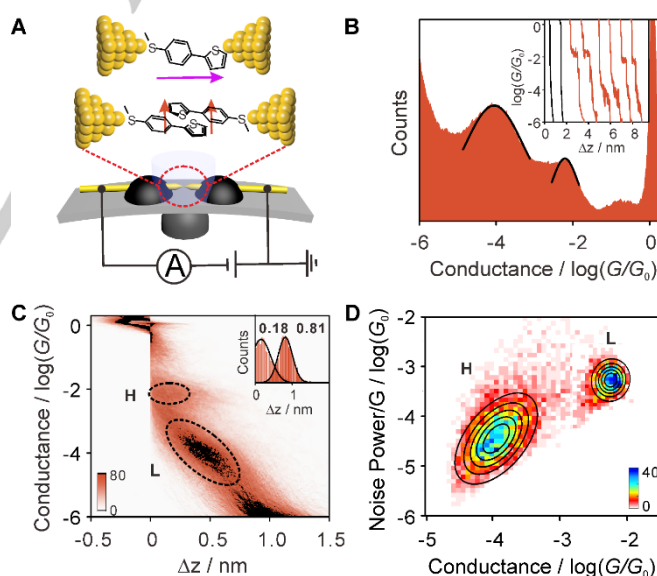

Figure 1. Conductance measurement of molecular junctions. (A) Schematic of the MCBJ technique and the illustration of single-molecule **S-T1** junction (upper) and single- stacking **S-T1** junction (bottom). (B) 1D conductance histograms and typical conductance-displacement traces (inset) of **S-T1** (red) and solvent (black). (C) 2D conductance histogram and the relative stretching displacement histograms from $10^{-0.3}$ G_0 to $10^{-2.8}$ G_0 of H state (0.18±0.03 nm, left inset) and $10^{-0.3}$ G_0 to $10^{-5.0}$ G_0 of L state (0.81±0.02 nm, right inset). The error bars are determined from the variations of the relative stretching displacement values in three independent conductance measurements. (D) 2D histogram of normalized flicker noise power versus average conductance of **S-T1**.

RESEARCH ARTICLE

To address how intermolecular charge transport through thiophene-stacking junctions vary among conjugation pattern, we synthesized another three kinds of thiophene-based derivatives i) molecules with increased thiophene units (**S-T2**, **S-T3**), ii) fused thiophene with more rigid structure (**S-TTT**) and iii) molecules with substituent groups on thiophene rings (**S-T1-Cl**, **S-T1-Br**). Figure 2 shows the 1D conductance histograms of the six thiophene derivatives. As shown in Figure 2A, **S-T2** and **S-T3** with two and three thiophene units each have only one conductance peak, and the conductance varies slightly from $10^{-4.05\pm0.04}$ G_0 (7.0±0.6 nS) to $10^{-3.91\pm0.03}$ G_0 (9.6±0.7 nS) compared with **S-T1** ($10^{-4.02\pm0.11}$ G_0). The stretching distances of these molecular junctions are significantly longer than calculated molecular lengths (see Figures S3A,B and Table S1). In addition, flicker noise analysis shows that the noise power scales as $G^{2.0}$ for **S-T2** and as $G^{1.6}$ for **S-T3** (Figures S3C,D), which are indicative of the through-space coupling through **S-T2** or **S-T3** dimers. Accordingly, we attribute the conductance peaks around $10^{-4.0}$ G_0 to single-stacking junctions of **S-T2** and **S-T3**. The absence of single-molecule junctions is possibly caused by the weak competitiveness compared with single-stacking junctions as the molecular conjugation length increase since the absence of single-molecule junctions and single-stacking junctions are competitive as discussed above. Then, the effects of substituent and different conjugation pattern on intermolecular charge transport were investigated. Interestingly, single-stacking junctions of **S-T1** derivatives with substituent groups, i.e., chlorine **S-T1-Cl** ($10^{-4.01\pm0.09}$ G_0, 7.7±1.6 nS) and bromine **S-T1-Br** ($10^{-4.07\pm0.02}$ G_0, 6.6±0.4 nS), and fused-ring thiophene **S-TTT** ($10^{-3.97\pm0.05}$ G_0, 8.3±0.9 nS) also show similar conductance values centered at $10^{-4.0}$ G_0 (Figure 2B), suggesting that charge transport ability through the single-stacking junctions based on thiophene units is nearly independent of the conjugation pattern. To explore the universality of the above findings, we extended the studies to benzene-based junctions with fused-ring from phenyl (**S-P1**) to naphthyl (**S-P2**) and to anthryl (**S-P3**) as shown in Figure S6. The conductance of **S-P1** ($10^{-4.34\pm0.01}$ G_0, 3.5±0.05 nS) and **S-P2** ($10^{-4.42\pm0.10}$ G_0, 3.0±0.7 nS) are similar but decrease apparently for **S-P3** ($10^{-4.60\pm0.08}$ G_0, 1.9±0.3 nS). Compared with thiophene system, the intermolecular charge transport ability of single-stacking junctions based on benzene units is generally lower. These results indicate that the thiophene-based single-stacking junctions exhibit excellent intermolecular charge transport ability, which is also more tolerant to the variation of molecular architecture.
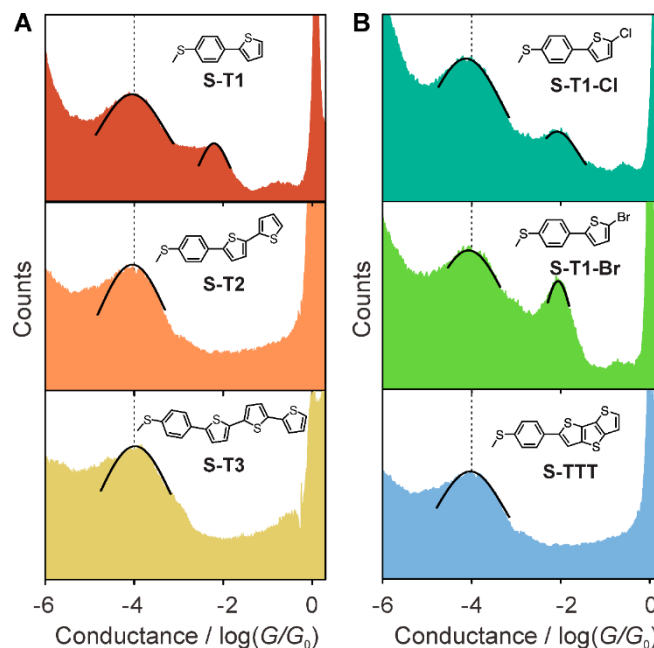

Figure 2. Investigation of intermolecular charge transport of thiophene derivatives. (A) Molecular structures and 1D conductance histograms of molecules **S-T1** ($10^{-4.02\pm0.11}$ G_0), **S-T2** ($10^{-4.05\pm0.04}$ G_0) and **S-T3** ($10^{-3.91\pm0.03}$ G_0) at 0.1 mM. (B) Molecular structures and corresponding 1D conductance histograms of **S-T1-Cl** ($10^{-4.01\pm0.09}$ G_0 and $10^{-2.01\pm0.03}$ G_0), **S-T1-Br** ($10^{-4.07\pm0.02}$ G_0 and $10^{-2.09\pm0.02}$ G_0) and **S-TTT** ($10^{-3.97\pm0.05}$ G_0). Detail analysis can be found in Figure S6.

Structure dependence of the stacking probability. Even though the conductance values of the single-stacking junctions remained nearly structure-independent, the conductance peaks, especially for benzene-based junctions (Figures S6D-F), become more pronounced as the conjugation region increases. This trend suggests that the structure of the conjugated core plays a role in the dynamic formation of single-stacking junctions. To evaluate the role of conjugation patterns in the intermolecular interactions quantitatively, we constructed displacement distribution histograms for **S-T1**, **S-T2** and **S-T3** at the conductance range between $10^{-(Gm-1)}$ G_0 and $10^{-(Gm+1)}$ G_0 (details in Supporting Information section 2.1). As illustrated in Figure 3A, the displacement distributions centered at 0.36 nm represent the direct tunneling feature without molecular junction (T), while the longer displacement distributions are assigned to single-stacking junctions (J). The area ratios of the relative stretching distance histograms obtained by Gaussian fitting reveal the formation percentage of single-stacking junctions. It was found that the stacking probability of thiophene-based junctions started from 80±0.9% (**S-T1**), increasing slightly to 83±1.0% for **S-T2** and 95±1.6% for **S-T3** (Figure 3B), which is attributed to the effective π-π stacking interactions arising from the increasing conjugated patterns. By contrast, the stacking probability of molecule **S-P1** was determined to be only 62±2.7%. When the π-conjugated core was expanded to yield the anthryl (**S-P3**), the stacking probability increased to a value as high as 91±3.9% (Figure 3B). The generally higher stacking probabilities of thiophene-based

RESEARCH ARTICLE

junctions are enhanced by the introduction of sulfur atoms, which introduce additional S-S[15] and S-π interactions[16] and increase the stability of the single-stacking junctions. Stacking probability analysis, together with the constant conductance of single-stacking junctions, provides essential insight into the charge transport enhancement induced by aggregation in organic semiconductors[3b] that aggregation increases the formation probability of short-range π-stacked units and subsequently leads to the enhanced charge transport through π-conjugated materials.
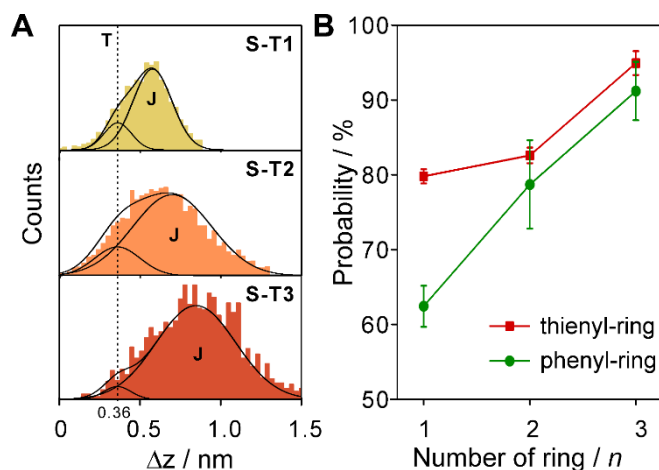

Figure 3. Structure dependence of the stacking probability. (A) The displacement distribution histograms of single-stacking junctions with molecules **S-T1**, **S-T2** and **S-T3** determined from $10^{-(Gm-1)}$ G_0 to $10^{-(Gm+1)}$ G_0. We refer to the direct tunneling feature as "T" (dashed black lines) and the molecular junction feature as "J". (B) Stacking probability as a function of the number of aromatic ring n without regard to p-phenylene connected with -SMe anchor group. The error bars are determined from the variations of the stacking probability in three independent conductance measurements.

The transition from intramolecular transport to intermolecular transport. As discussed above, the charge transport through thiophene-based single-stacking junctions can be detected using MCBJ technique, providing the opportunity to explore the intermolecular and intramolecular charge transport, (as shown in Figure 4A), through thiophene derivatives at the single-molecule level. To distinguish the intermolecular and intramolecular charge transport, our approach was to investigate charge transport through single-stacking and single-molecule junctions with the same thiophene backbone. As shown in Figure 4B, the molecules in orange with only one -SMe terminal were employed to form a single-stacking junction as we have discussed, and the intramolecular charge transport through the thiophene backbones was investigated using the molecule in purple with both –SMe terminals bridged between two gold electrodes.

Different from the structure-independent conductance of single-staking junctions, the conductance of single-molecule junctions decreased significantly from $10^{-3.43\pm0.10}$ G_0 (29.5±6.9 nS, **S-T1-S**) to $10^{-3.78\pm0.05}$ G_0 (12.8±0.2 nS, **S-T2-S**), as shown in Figure 4C. For **S-T3-S**, significant concentration-dependence is observed

with the conductance increasing from $10^{-4.31\pm0.07}$ G_0 (3.8±0.6 nS, 0.001 mM) to $10^{-3.89\pm0.05}$ G_0 (9.9±1.2 nS, 0.1 mM), as shown in Figure 4D. Figure 4E shows the 2D conductance-distance histogram and electronic coupling through flicker noise analysis of **S-T3-S** at 0.1 mM. The noise power scales as $G^{1.6}$ for **S-T3-S**, indicating that the charge transport through **S-T3-S** was through-space-dominated at higher concentration. Furthermore, the concentration-dependent fluorescence emission spectra of **S-T3-S** reveal that monomer prevails below 0.01 mM and begins to aggregate from 0.01 mM to 0.1 mM (Figure S8), indicating that the conductance at low concentration of 0.001 mM and high concentration of 0.1 mM could be assigned to single-molecule junctions and single-stacking junctions, respectively. Therefore, the **S-T3-S** will undergo the transition from single-molecule to single-stacking at higher concentration. The concentration-dependent behavior of **S-T3-S** found here is different from that of oligothiophene reported by Capozzi et al.[7b] The discrepancy was possibly attributed to the structural difference between oligothiophene and the thiophene/phenylene co-oligomer which forms intermolecular complexes with the increasing concentrations.[17] However, no concentration dependence was observed for short molecules like **S-T2-S**, and the corresponding noise power scale as $G^{1.2}$ for 0.1 mM. These results demonstrated that the charge transport paths between intermolecular and intramolecular could be controlled by rational molecular design. Long conjugation structure is more favorable for the construction of intermolecular charge transport, because of the strong molecular interactions.

Figure 4F summarised the conductance evolution of single-stacking (dashed line) and single-molecule (solid line) junctions varying with molecular length. The single-molecule conductance of **S-T1-S**, **S-T2-S** and **S-T3-S** decrease exponentially with the increasing thiophene units, which is consistent with the conductance decay of single-molecule oligothiophene junctions[7a, 7b] and DFT calculations (Figure S11J). In contrast, the conductance of single-stacking junctions is almost unchanged. When the molecules are relatively short, the conductance of single-stacking junctions is lower than those of corresponding single-molecule junctions. However, there is a reversal when the conjugation pattern increased to three thiophene rings that the single-stacking conductance of **S-T3** is ~200% higher than the single-molecule conductance of **S-T3-S**, suggesting the intermolecular charge transport is even more efficient than intramolecular charge transport with large conjugation patterns. The conductance transition originates from the significant conductance decay with length of intramolecular charge transport and the near length-independence of intermolecular charge transport through single-stacking junctions. Such low length decay of through-space charge transport is also found in single-stacking junctions based on benzene (Figure S7P) and previous report about π-folded molecular junctions based on anthracene moieties[18].
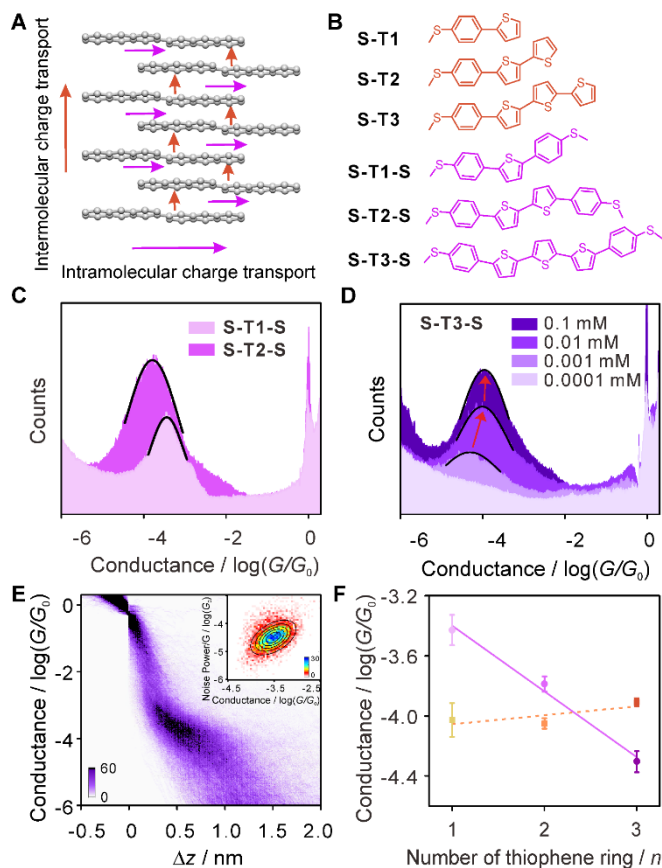
RESEARCH ARTICLE

Figure 4. Investigation of intermolecular and intramolecular charge transport. (A) Schematic illustration of intramolecular and intermolecular charge transport. (B) Molecular structures used for comparison. (C) 1D conductance histograms of **S-T1-S** and **S-T2-S**. (D) 1D conductance histograms of **S-T3-S** at different concentrations. (E) 2D conductance histograms and 2D histogram of normalized flicker noise power versus average conductance of **S-T3-S** at 0.1 mM. (F) The conductance as a function of the number of thiophene ring n in single-molecule (solid line) and single-stacking (dotted line) junctions at 0.1 mM except for **S-T3-S** at 0.001 mM. The error bars are determined from the variations of the most probable conductance values in three independent conductance measurements.

Theoretical investigation of the transmission function and stacking energy. To understand the intermolecular-dominated charge transport, we further calculated the transmission function $T(E)$ describing electrons of energy E passing from one electrode to the other using a combination of the software package SIESTA[19] based on *ab initio* DFT and the quantum transport code Gollum.[20] To model the evolution of the single-stacking junction, two target molecules were initially attached to two gold pyramidal-shaped electrodes, as shown in Figure 5A (upper) for molecule **S-T1**. Then, the electrode spacing d was increased gradually in increments of 0.05 nm, from $d = 1.52$ nm to the break-off distance of the π-stacked dimers, as shown in Figure 5A (bottom). Figure 5B shows examples of the transmission functions of a single-stacking **S-T1** junction at various stages of the stretching simulation (details in Figure S11A). The transmission curves demonstrate that both constructive and destructive quantum interference are observed during the

stretching process. However, only the high conductance state was obtained in our experiments due to the relatively high stretching rate, which is in accordance with the previous report.[21] Figure 5C show the room-temperature conductance evolutions during stretching obtained from the transmission coefficients at the Fermi level estimated by DFT. During junction stretching, oscillations in conductance occur, as theoretically predicted[22] and measured[21] in previous works, and the conductance histograms (inset of Figure 5C) suggest that the calculated conductance of dimers is approximately $10^{-5.0}$ G_0. The similar conductance regions among different derivatives and variation tendency provide qualitative theoretical evidence for the conductance consistency observed experimentally.
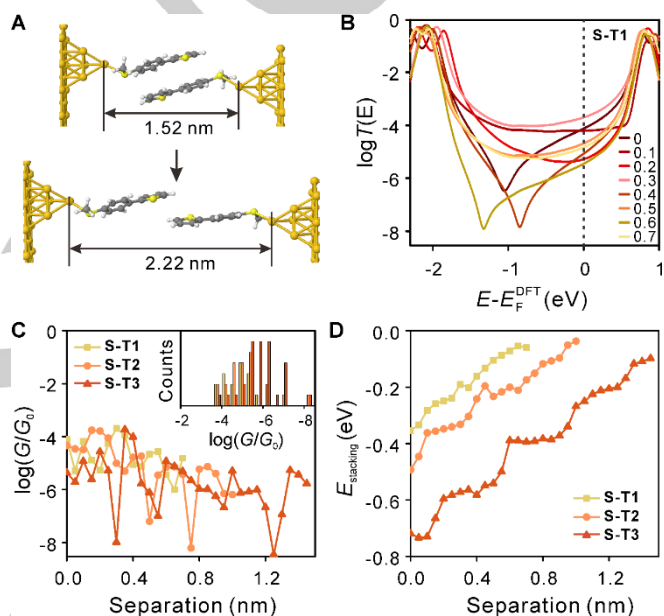

Figure 5. Transmission curves and stacking energies calculated between single-stacking junctions. (A) Schematics of the stretching simulation from full-stacking (1.52 nm) to zero-stacking (2.22 nm) of **S-T1** junction. (B) Representative transmission curves of single-stacking **S-T1** junction at different separation distance between two π-stacked dimer, where "0" is the initial full-stacking state, and increases in increments of 0.1 nm until to zero-stacking state ("0.7"). (C) The corresponding conductance evolutions obtained from the transmission coefficients at the Fermi level versus separation distance of **S-T1**, **S-T2** and **S-T3** and the conductance histograms (inset) with a bin size of 0.4 log(G/G_0). (D) Stacking energies calculated between dimers of molecule **S-T1**, **S-T2** and **S-T3** versus the relative separation distance between two gold electrodes.

To investigate the effect of molecular structure on the stacking probability, we also calculated the stacking energy of the dimers in the junctions at each increment of the stretching process. As shown in Figure 5D, the binding energies (see Supporting Information) decrease almost monotonically as the separation distance d increases. The initial binding energy for thiophene-based **S-T1** is lower than that of **S-T2** and **S-T3**, because the area of the initial π-π overlap area of **S-T1** is smaller than the initial overlap areas of **S-T2** and **S-T3**. This feature supports our experimental results indicating that the binging probability of **S-T1**

RESEARCH ARTICLE

is lower than that of **S-T2** and **S-T3**. Since the measured stacking probabilities follow the trends observed for the initial binding energies, it is inferred that the structure dependence of the stacking probability originates from variations in the binding energies of the π-π stacking.

Conclusion

In conclusion, we investigated the intermolecular and intramolecular charge transport properties in single-molecule and single-stacking thiophene junctions using MCBJ technique. We demonstrated that the conductance of thiophene-based single-stacking junctions is nearly independent of the conjugated pattern and the dominant charge transport path transits from intramolecular to intermolecular paths when the conjugation pattern increased. We also found that the major effect from the increased conjugated region is to improve the dynamic formation process of single-stacking junction rather than its intrinsic conductance at molecular level. The results were further confirmed by the theoretical calculations, which predict similar conductance tendencies and different binding energies of the single-stacking junctions. Our results not only provides the fundamental understanding of structure-property relationship but also offer fundamental insight into how, from a single-molecule perspective, microscopic charge transport in highly disordered materials enables existing aggregation to increase the formation probability of intermolecular charge transport channels. We believe our findings will inspire various new design strategies for the fabrication of high-performance organic devices *via* molecular engineering of intermolecular interactions.

Acknowledgments

Keywords: thiophene • single-stacking junction • mechanically controllable break junction • structure-independent conductance• intermolecular charge transport

[1]   a) S. Wang, J. Xu, W. Wang, G.-J. N. Wang, R. Rastak, F. Molina-Lopez, J. W. Chung, S. Niu, V. R. Feig, J. Lopez, T. Lei, S.-K. Kwon, Y. Kim, A. M. Foudeh, A. Ehrlich, A. Gasperini, Y. Yun, B. Murmann, J. B. H. Tok, Z. Bao, *Nature* **2018**, *555*, 83-88; b) C. Jiang, H. W. Choi, X. Cheng, H. Ma, D. Hasko, A. Nathan, *Science* **2019**, *363*, 719-723; c) H. Sirringhaus, *Adv. Mater.* **2014**, *26*, 1319-1335.

[2]   a) V. Coropceanu, J. Cornil, D. A. da Silva Filho, Y. Olivier, R. Silbey, J.-L. Brédas, *Chem. Rev.* **2007**, *107*, 926-952; b) Y. Diao, B. C. K. Tee, G. Giri, J. Xu, D. H. Kim, H. A. Becerril, R. M. Stoltenberg, T. H. Lee, G. Xue, S. C. B. Mannsfeld, Z. Bao, *Nat. Mater.* **2013**, *12*, 665-671; c) Z. Shuai, H. Geng, W. Xu, Y. Liao, J.-M. André, *Chem. Soc. Rev.* **2014**, *43*, 2662-2679; d) C. Wang, H. Dong, L. Jiang, W. Hu, *Chem. Soc. Rev.* **2018**, *47*, 422-500.

[3]   a) J. Hou, O. Inganäs, R. H. Friend, F. Gao, *Nat. Mater.* **2018**, *17*, 119; b) R. Noriega, J. Rivnay, K. Vandewal, F. P. V. Koch, N. Stingelin, P. Smith, M. F. Toney, A. Salleo, *Nat. Mater.* **2013**, *12*, 1038; c) J. Mei, Y. Diao, A. L. Appleton, L. Fang, Z. Bao, *J. Am. Chem. Soc.* **2013**, *135*, 6724-6746; d) X. Guo, A. Facchetti, T. J. Marks, *Chem. Rev.* **2014**, *114*, 8943-9021; e) H. Zang, Y. Liang, L. Yu, B. Hu, *Advanced Energy Materials* **2011**, *1*, 923-929.

[4]   J. L. Brédas, J. P. Calbert, D. A. da Silva Filho, J. Cornil, *Proc. Nat. Acad. Sci. U.S.A.* **2002**, *99*, 5804-5809.

[5]   a) S. Wu, M. T. Gonzalez, R. Huber, S. Grunder, M. Mayor, C. Schoenenberger, M. Calame, *Nat. Nanotech.* **2008**, *3*, 569-574; b) S. Martin, I. Grace, M. R. Bryce, C. Wang, R. Jitchati, A. S. Batsanov, S. J. Higgins, C. J. Lambert, R. J. Nichols, *J. Am. Chem. Soc.* **2010**, *132*, 9157-9164.

[6]   a) A. Mishra, C.-Q. Ma, J. L. Segura, P. Bäuerle, in *Handbook of Thiophene-Based Materials*, John Wiley & Sons, Ltd, **2009**, pp. 1-155; b) M. E. Cinar, T. Ozturk, *Chem. Rev.* **2015**, *115*, 3036-3140; c) J.-S. Ni, P. Zhang, T. Jiang, Y. Chen, H. Su, D. Wang, Z.-Q. Yu, R. T. K. Kwok, Z. Zhao, J. W. Y. Lam, B. Z. Tang, *Adv. Mater.* **2018**, *30*, 1805220.

[7]   a) L. Xiang, T. Hines, J. L. Palma, X. Lu, V. Mujica, M. A. Ratner, G. Zhou, N. Tao, *J. Am. Chem. Soc.* **2016**, *138*, 679-687; b) B. Capozzi, E. J. Dell, T. C. Berkelbach, D. R. Reichman, L. Venkataraman, L. M. Campos, *J. Am. Chem. Soc.* **2014**, *136*, 10486-10492; c) S. K. Lee, R. Yamada, S. Tanaka, G. S. Chang, Y. Asai, H. Tada, *ACS Nano* **2012**, *6*, 5078-5082; d) B. Q. Xu, X. L. Li, X. Y. Xiao, H. Sakaguchi, N. J. Tao, *Nano Lett.* **2005**, *5*, 1491-1495; e) E. Leary, H. Höbenreich, S. J. Higgins, H. van Zalinge, W. Haiss, R. J. Nichols, C. M. Finch, I. Grace, C. J. Lambert, R. McGrath, J. Smerdon, *Phys. Rev. Lett.* **2009**, *102*, 086801.

[8]   A. I. Yanson, G. R. Bollinger, H. E. van den Brom, N. Agraït, J. M. van Ruitenbeek, *Nature* **1998**, *395*, 783.

[9]   a) M. Wawrzyniak, J. Martinek, B. Susla, G. Ilnicki, *Acta Phys. Pol., A* **2009**, *115*, 384-386; b) A. Halbritter, P. Makk, S. Mackowiak, S. Csonka, M. Wawrzyniak, J. Martinek, *Phys. Rev. Lett.* **2010**, *105*, 266805; c) A. Mishchenko, L. A. Zotti, D. Vonlanthen, M. Bürkle, F. Pauly, J. C. Cuevas, M. Mayor, T. Wandlowski, *J. Am. Chem. Soc.* **2011**, *133*, 184-187; d) P. Makk, D. Tomaszewski, J. Martinek, Z. Balogh, S. Csonka, M. Wawrzyniak, M. Frei, L. Venkataraman, A. Halbritter, *Acs Nano* **2012**, *6*, 3411-3423.

[10]   A. C. Aragonès, N. Darwish, J. Im, B. Lim, J. Choi, S. Koo, I. Díez-Pérez, *Chem. - Eur. J.* **2015**, *21*, 7716-7720.

[11]   C. R. Arroyo, S. Tarkuc, R. Frisenda, J. S. Seldenthuis, C. H. M. Woerde, R. Eelkema, F. C. Grozema, H. S. J. van der Zant, *Angew. Chem. Int. Edit.* **2013**, *52*, 3152-3155.

[12]   W. Hong, D. Z. Manrique, P. Moreno-Garcia, M. Gulcur, A. Mishchenko, C. J. Lambert, M. R. Bryce, T. Wandlowski, *J. Am. Chem. Soc.* **2012**, *134*, 2292-2304.

[13]   a) A. Magyarkuti, O. Adak, A. Halbritter, L. Venkataraman, *Nanoscale* **2018**, *10*, 3362-3368; b) M. H. Garner, H. Li, Y. Chen, T. A. Su, Z. Shangguan, D. W. Paley, T. Liu, F. Ng, H. Li, S. Xiao, C. Nuckolls, L. Venkataraman, G. C. Solomon, *Nature* **2018**, *558*, 415.

[14]   L. Xiang, T. Hines, J. L. Palma, X. Lu, V. Mujica, M. A. Ratner, G. Zhou, N. Tao, *J. Am. Chem. Soc.* **2016**, *138*, 679-687.

[15]   R. Gleiter, G. Haberhauer, D. B. Werz, F. Rominger, C. Bleiholder, *Chem. Rev.* **2018**, *118*, 2010-2041.

[16]   S. K. Rajagopal, P. S. Salini, M. Hariharan, *Crystal Growth & Design* **2016**, *16*, 4567-4573.

[17]   S. A. Lee, S. Hotta, F. Nakanishi, *J. Phys. Chem. A* **2000**, *104*, 1827-1833.

[18]   M. Carini, M. P. Ruiz, I. Usabiaga, J. A. Fernández, E. J. Cocinero, M. Melle-Franco, I. Diez-Perez, A. Mateo-Alonso, *Nat. Commun.* **2017**, *8*, 15195.

[19]   A. R. Rocha, V. M. García-suárez, S. W. Bailey, C. J. Lambert, J. Ferrer, S. Sanvito, *Nat. Mater.* **2005**, *4*, 335.

[20]   J. Ferrer, C. J. Lambert, V. M. Garcia-Suarez, D. Z. Manrique, D. Visontai, L. Oroszlany, R. Rodriguez-Ferradas, I. Grace, S. W. D. Bailey, K. Gillemot, H. Sadeghi, L. A. Algharagholy, *New J. Phys.* **2014**, *16*.

[21]   R. Frisenda, V. A. E. C. Janssen, F. C. Grozema, H. S. J. van der Zant, N. Renaud, *Nat. Chem.* **2016**, *8*, 1099-1104.

[22]   M. K. Al-Khaykanee, A. K. Ismael, I. Grace, C. J. Lambert, *RSC Advances* **2018**, *8*, 24711-24715.

WILEY-VCH

RESEARCH ARTICLE

RESEARCH ARTICLE

We demonstrated that the conductance of thiophene-based single-stacking junctions is nearly independent of the conjugated pattern that the dominant charge transport path transits from intramolecular to intermolecular paths when the conjugation pattern increased.

Intermolecular vs Intramolecular Charge Transport
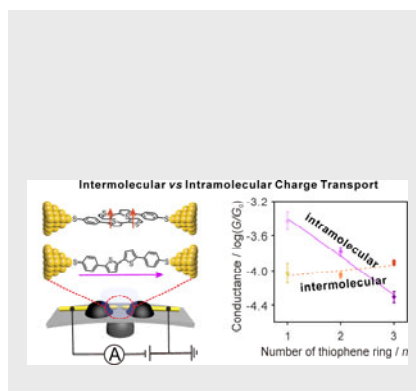
Xiaohui Li, Qingqing Wu, Jie Bai, Songjun Hou, Wenlin Jiang, Chun Tang, Hang Song, Xiaojuan Huang, Jueting Zheng, Yang Yang, Junyang Liu, Yong Hu, Jia Shi, Zitong Liu,* Colin J. Lambert,* Deqing Zhang,* Wenjing Hong*

Page No. – Page No.

Structure-Independent Conductance of Thiophene-Based Single-Stacking Junctions

Accepted Manuscript